

Scalable Fe₂O₃-NiO Oxygen Carrier for Dual-stage Hydrogen Production from Mid-temperature Methane Chemical Looping Steam Reforming

Sanli Tang¹, Zhongrui Gai^{1,2}, Yang Li^{1,3}, Yunlian Liu^{1,3}, Mingkai Liu^{1,3}, Ying Pan^{1*,3}

1 Institute of Engineering Thermophysics, Chinese Academy of Sciences, Beijing 100190, China

2 State Key Laboratory of Multiphase Flow in Power Engineering, Xi'an Jiaotong University, Xi'an 710049, China

3 University of Chinese Academy of Sciences, Beijing 100049, China

(*Corresponding Author: panying@iet.cn)

ABSTRACT

Methane chemical looping has emerged as a promising avenue to produce blue or green hydrogen. Among the various oxygen carriers investigated for this process, Fe₂O₃ and NiO have garnered significant attention due to their affordability and non-toxic nature. However, the utilization of such oxygen carriers has exhibited satisfactory yields only at temperatures exceeding 800 °C. This limitation poses challenges for industrial reactor design and application. In this study, we present a novel approach involving the design of nanoscale Fe/Ni bimetallic oxygen carriers. This strategic design can reach a deeper reduction state to FeO while reducing the temperature to 500-600 °C. Moreover, we have achieved scalable production of the proposed oxygen carrier, with a negligible penalty in CH₄ conversion (<3%) compared to laboratory-scale samples. A typical 10-kg scale nano oxygen carrier maintained a H₂ purity of >78% in the outlet and stable performance over 300 cycles. Such noteworthy findings contribute to the advancement of chemical looping plants for green hydrogen production and refueling.

Keywords: Mid-temperature dual-stage chemical looping reforming, Blue H₂ production, Bimetallic oxygen carrier

1. INTRODUCTION

Chemical looping methane reforming is a promising H₂ generation process under moderate condition with a possibility of economic CO₂-capture [1, 2]. The methane reforming at 900 °C was firstly reported using Ni or Fe based oxygen carrier [3]. As the focus of research, the oxygen carrier has been studied on its characters like

anti-coking, anti-sintering, and lower energy barrier when forming CO and H₂ [4-6]. Another focus was to achieve a deeper extent of reduction on the oxygen carrier, in order to promote H₂ generation. The fully reduced FeO and Fe can react with H₂O, forming hydrogen in both steps of the chemical looping reforming cycle [7, 8].

As an improvement, bimetallic oxygen carrier was proposed to achieve a deeper reduction extent of the oxygen carrier, therefore a potentially higher H₂ concentration [9]. On a Fe-Ni bimetallic oxygen carrier, the methane firstly reduced NiO to Ni.[10] The metallic Ni acted as a catalyst for both CH₄ cracking and reforming, which generated H₂ and reduced Fe₂O₃ to FeO. The reducing potential of FeO enabled H₂ generation from H₂O or CO generation from CO₂ in the oxidation step, improving the H₂ generation rate of the whole cycle. Another improvement of bimetallic oxygen carrier was the reaction selectivity. A Ce-Fe bimetallic realized resilient shift of the H₂/CO ratio from 1 to 4, which can satisfy the need of either organic synthesis (syngas product) or power generation in a fuel cell (high H₂ and low CO concentration). Even on the surface of a commercial Fe₂O₃ sample, the loading of NiO has proven promising in chemical looping gasification of biofuels.[11]

The key to performance improvement in bimetallic oxygen carrier is the synergy of the metallic species during the reaction pathway.[12] Theoretically, a finer blend of the metallic species usually contains synergetic effects of alloy, leading to more ideal H₂ generation or a favored H₂/CO ratio.[13] To approximate such goal, the idea of co-growth can be employed as bottom-to-top growth of metal oxide nanocrystals. One of the most viable methods is hydrothermal synthesis. Such method

started from a co-precipitation of metal hydroxide precursors, following hydrothermal growth of metal oxide crystal. By altering the condition of hydrothermal process, the shape, phase, and size of the oxygen carrier can be controlled. As indicated by its high sensitivity as a probe [14] or an electrode material,[15] reducing the size of Fe₂O₃/NiO to nanocrystals can be potentially beneficial to its reactivity. This has shed light on the design of nanoscale Fe-Ni bimetallic oxygen carrier for mid-temperature two-grade chemical looping hydrogen production.

Another gap in the bimetallic oxygen carrier is the mass production of nanoscale oxygen carrier. Usually, when expanding the scale of synthesis, it's hard to control the temperature, pressure and concentration conditions exactly the same as those under laboratory scale synthesis [16]. However, such conditions are crucial for the hydrothermal process by influencing the structuring and re-shaping of nano-crystals and the migration and co-precipitation of metallic species.[17] It's necessary to propose a rational design of scalable synthetic method, reactor and work flow for accelerating the industrialization of nanoscale bimetallic oxygen carrier.

In this study, we proposed a nanoscale Fe-Ni bimetallic oxygen carrier for two-grade hydrogen production from methane chemical looping reforming. The oxygen carrier benefits from the exchange of H₂ and carbonated species between Fe and Ni species, thus reducing the temperature to 600 °C while achieving a highest methane conversion above 94% and a highest H₂/CH₄ ratio above 4. Using CO₂ absorber, the methane was close to a fully conversion and the H₂/CH₄ ratio can be further promoted to above 2.5. Furthermore, a scaled production was designed and setup for the proposed oxygen carrier, realizing kg-scale production of the proposed nano scale oxygen carrier. The scaled synthesized oxygen carrier kept the performance of lab-scale samples, with a performance reduction of <3%.

The aim of this study is to develop and apply the nanoscale Fe-Ni bimetallic oxygen carrier for scalable, pure and low-temperature hydrogen production from a highly-efficient methane chemical looping reforming process. Essential characterizations would be provided for reaction mechanism as the explanations for elevated performance, as well as the criterions for qualified, scale-synthesized oxygen carriers in future research.

2. METHODS

2.1 Laboratory scale synthesis

All reagents were of analytical grade and used without further purification. In the experiment, 5 g of Fe(NO₃)₃·9H₂O and 1.2 g of Ni(NO₃)₂·6H₂O were dissolved into a mixture of 51 ml distilled water, 5 mL ethylene glycol and 4 g Al₂O₃ nanoparticles. Then, 8 mol L⁻¹ NaOH solution was added under vigorous stirring to adjust pH value to 9-9.5. After being stirred for 15 min, the solution was transferred into a 100-mL Teflon-lined stainless-steel autoclave. The autoclave was maintained at 120 °C for 10 h then cooled to room temperature. Finally, the products were washed with distilled water and absolute ethanol for three times and dried at 80 °C for 12 h. The samples were ball-milled then an oxygen carrier powder in a dark red color was acquired.

2.2 Laboratory scale synthesis

We doubled the concentration of Fe(NO₃)₃·9H₂O and Ni(NO₃)₂·6H₂O solution and expanded the reaction scale for 100 times to acquire kg-level production of oxygen carriers. A high-pressure reactor was built with an operating pressure range at 0.05-25 atm and temperature range at 0-200 °C. The stirring was maintained at 900 rpm during co-precipitation process while at 90 rpm during the hydrothermal reaction process. The other operating parameters were the same as those in the laboratory scale. After the hydrothermal synthesis, a full industrial work flow of centrifugal-washing, drying and ball-milling was followed to acquire a similar oxygen carrier power as that in laboratory scale synthesis.

2.3 Reference oxygen carrier

The reference sample was made by the mechanical blend of α-Fe₂O₃, NiO and Al₂O₃ nanoparticles (both 99.9% metal basis) purchased from Alfar. The molar ratio of each element was the same as that in the aforementioned synthesis step.

2.4 Methane chemical looping reforming condition

The reaction was conducted in fixed bed reactor with 0.4 g oxygen carrier under a temperature range of 500-600 °C (25 °C a point) and atmospheric pressure. In default setting, the reduction reaction lasted 10 min, with inlet gas flow of 10 sccm consisting of 1:6 CH₄ and Ar. Water steam was brought into the reactor by the inlet gas, maintaining a molar ratio of H₂O and CH₄ (S/C ratio) at 0.8:1. The oxidation reaction was followed until no H₂ was released from the oxygen carrier. Experiments on sensitivity would be further carried out by changing the reduction time and S/C ratio in the default setting.

3. RESULTS AND DISCUSSION

3.1 Characterizations of the lab-scale and 10-kg scale sample

XRD, SEM and EDX were done for as-synthesized samples. According to XRD spectra (Fig. 1a), both oxygen carriers exhibited poor crystallinity, though the 10-kg scale had a stronger peak intensity. This is typical for hydrothermal synthesis which tends to form of small or amorphous Fe_2O_3 and NiO nanoparticles with weaker XRD peaks [18]. The SEM image (Fig. 1b) showed both oxygen carrier was μm -scale, porous chunks of oxygen carrier consisting of ~ 100 nm nanoparticles of $\text{Fe}_2\text{O}_3/\text{NiO}$. This provided a possibility for the co-operation of bimetallic oxygen carrier species.

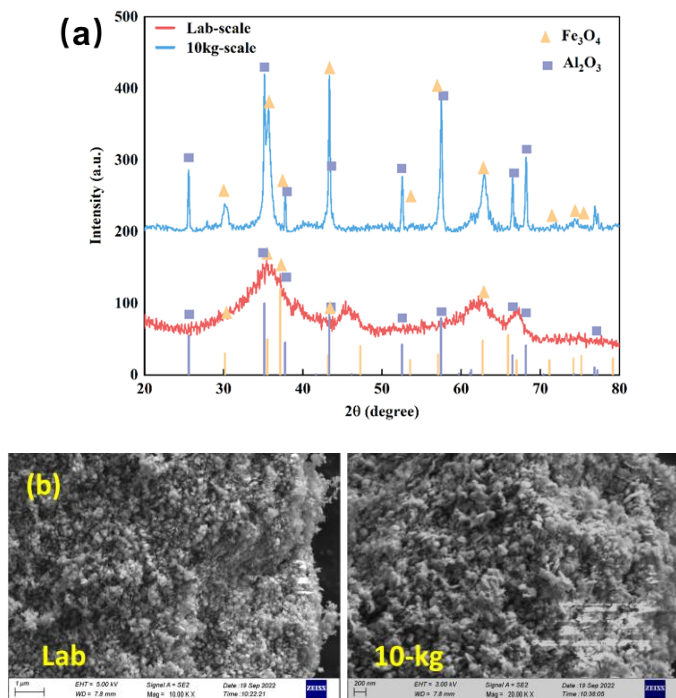


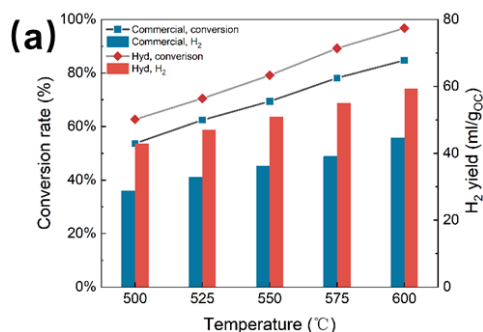
Fig. 1 Comparison of the (a) XRD spectra and (b) SEM images of the fresh sample from laboratory scale (left) and 10-kg scale (right). The scale bar in SEM image is 400 nm.

3.2 Mid-temperature dual-stage CLR reaction activity

Methane conversion rates and hydrogen production performance were averaged on 3 consecutive cycles and depicted in Fig. 2a. Generally, the conversion rate and hydrogen production rate increased as temperature went up. It should be noted that at above 575 °C, a conversion rate > 94 % and hydrogen production > 56 mL/g of a whole cycle can be acquired. The highest performance was achieved at 600 °C, with 98 % conversion rate and 59 mL/g of H_2 yield. Even the

temperature was reduced to 500 °C, the hydrogen yield was still above 46 mL/g. By comparison with the reference of Fe_2O_3 and NiO blend (the blue bars), we found that the nanoscale co-existence of Fe-Ni bimetallic species can better approach the equilibrium conversion rate and a high H_2 productivity.

Specially in Fig. 2b, we monitored the real-time contents of gaseous products in a single cycle at 600 °C. In the early stage of reduction, there was a surge of CO_2 and CO products from CH_4 full and partial oxidization by the oxygen carrier. The CO_2 concentration grew faster and achieved the peak earlier than CO , which indicated a typical bimetallic oxygen carrier reaction mechanism: the NiO was firstly reduced, producing Ni nanoparticles and CO_2 . The Ni metal is a decent catalyst for CH_4 cracking into H_2 , during which the coking can be eliminated by steam. This resulted in a surge of H_2 concentration at 100-420 s. Simultaneously, H_2 is the main activator of Fe_2O_3 chemical looping reaction,[19] therefore starting the reduction of Fe_2O_3 by CH_4 to a mixture of Fe_3O_4 and FeO . During this stage, the CO_2 remained a plateau while the H_2 production rate nearly doubled. The extra H_2 was from water which joined the reaction between Fe_2O_3 and CH_4 . During the reduction, the outlet had a CH_4 conversion of 95%, H_2 concentration of 75-78 % and CO_2 concentration of 10-20 %. In the oxidation stage, the H_2 concentration was 60-75 % plus CO_2 concentration of 10-20 %. One reason of the CO_2 appearance was the residual from the reduction stage, another reason is the water reacting with coke. Considering a 1:2 ratio for coke to H_2 from water, there was still over 60 % H_2 from water oxidation of FeO or Fe_3O_4 , indicating a fuel utilization comparable to traditional CH_4 reforming.



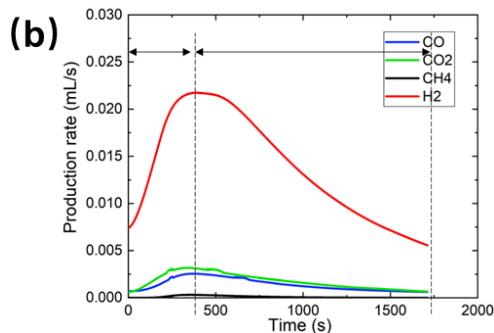


Fig. 2 (a) Comparison between lab-scale and commercial blend oxygen carrier. (b) Concentration of the gaseous outlet in one typical cycle.

3.3 Performance of the 10-kg scale sample

In the same reaction conditions, we examined the performances of the oxygen carrier synthesized in 10-kg level. In a typical cycle (Fig. 3a), the H₂ produced from the oxidation step was 1/4 of that from the reduction step. For the stability of reaction activity, we conducted a repeated experiment of 5 consecutive cycles for the 10-kg scale nano oxygen carrier (Fig. 3b and c). Through the 5 cycles under 600 °C, the CH₄ conversion, H₂ purity and H₂ production rate maintained stable. Over 91% CH₄ was converted, reaching a near-equilibrium conversion rate which surpassed CH₄ reforming. Especially, a >78% purity of H₂ can be acquired at a rate of 8 mL/min/g_{oc} in the reaction outlet, which is beneficial for reducing the gas separation cost in industrial CH₄ reforming. In a whole cycle, a total amount of 50 mL H₂ can be generated per gram of oxygen carrier. To sum up, the penalty from lab-scale oxygen carrier was below 3% in CH₄ conversion rate and total H₂ yield.

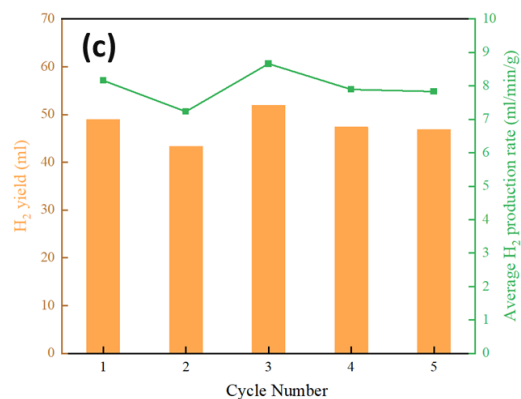
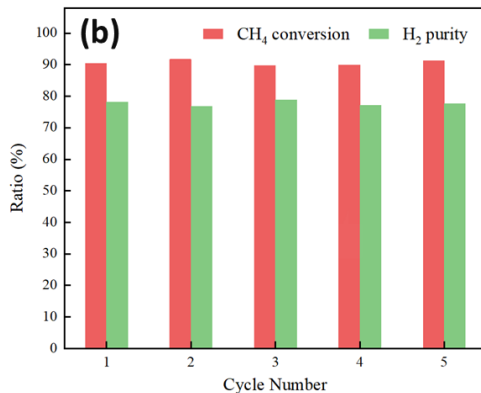
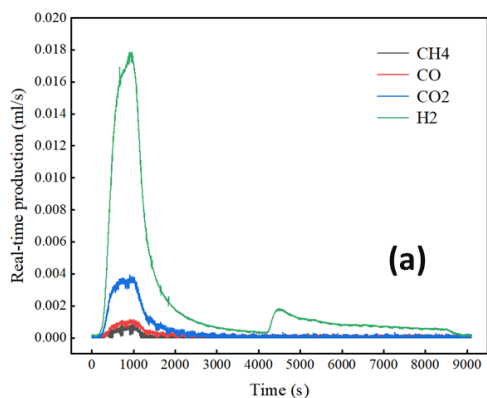


Fig. 3 (a) The concentration of gaseous outlet in one typical cycle of the 10-kg scale oxygen carrier. The inset shows the TG curve in reduction reaction. (b) The CH₄ conversion, H₂ purity, (c) total H₂ yield and H₂ production rate in 5 consecutive cycles. All reactions were done under 600 °C and a steam flow of 5 μL/min.

3.4 Sensitivity to S/C ratio

By changing the steam/CH₄ (S/C) molar ratio, the methane conversion rate and hydrogen production ratio can be tuned for different application scenarios. When S/C = 1, the methane conversion rate was below 90% in the reduction stage, and each CH₄ can produce over 2 H₂ molecules. When S/C = 5, each CH₄ produced 3.6 H₂ and the methane conversion rate was over 93%. Though the vaporization of water consumed a considerable amount of energy, increasing the S/C ratio can help approach a performance similar to the steam reforming of CH₄ but under a moderate temperature of 600 °C.

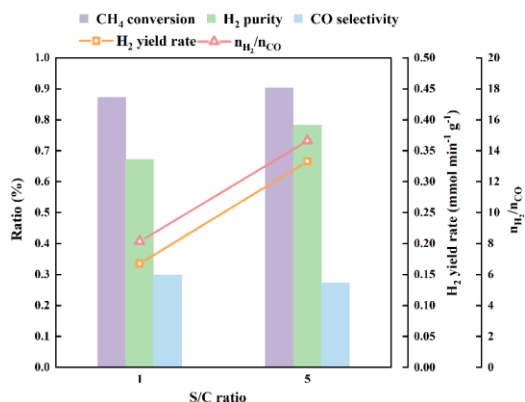


Fig. 4 The sensitivity to S/C ratio with different preference to CH₄ conversion or H₂ production.

3.5 Stability and longevity

We examined the long-term cyclic stability of laboratory and scale-produced nano oxygen carrier. A 60-cycle consecutive TG test was done under 600 °C (Fig. 5a), where the reduction lasted 20 min and the water steam was replaced by CO₂ during oxidization. It can be seen that in the beginning, there existed an activation stage where the mass loss continued increasing for several cycles. After 5 cycles, the mass loss stabilized at and averaged value of 4.95%, indicating the deep reduction from Fe₂O₃ to Fe₃O₄ and FeO.

In long-term cyclic test, sintering and phase separation of the bimetallic nano oxygen carrier was usually reported. As a result, the sample after 300 cycles were examined under XRD, SEM and EDX for morphology and elementary mapping. By comparing the XRD phases of the fresh and cycled oxygen carriers (Fig. 5b), a stable α -Fe₂O₃ phase was found to form after 5 cycles under 600 °C, sustaining a stable reactivity.

From SEM image, one can find that the fresh sample had nanosheet morphology, which was transformed into nanoparticles in used samples (Fig. 5c). This results from the re-crystallization of Fe₂O₃ and NiO in the repeated reduction and oxidation. Though the morphology has changed from near-amorphous to crystalline, no obvious sintering was found in the used sample, indicating nanocrystals of Fe₂O₃ and NiO. Furthermore, the elemental mapping from EDX has revealed homogeneous distribution of Fe and Ni elements both in the fresh sample and the sample after 300-cycles (Fig. 5d). Since no localized enrichment of either element was found, the bimetallic Fe-Ni oxygen carrier can be evidenced as phase separation free. Such long-term stability sustained the potential industrialization of the scalable bimetallic nano oxygen carrier.

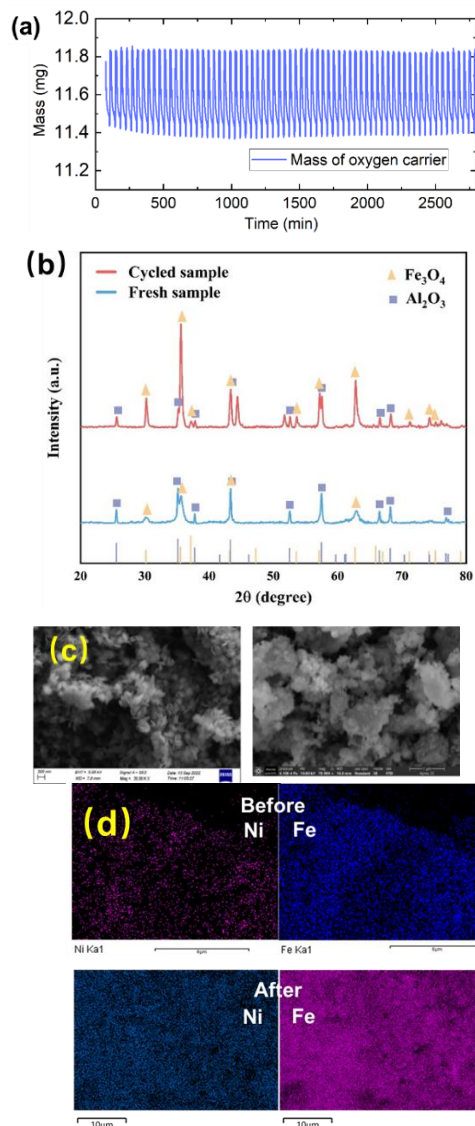


Fig. 5 (a) A 60-cycle consecutive TG test of the 10-kg scale oxygen carrier. (b) Comparison of XRD spectra of the fresh and cycled samples, the latter one had a higher crystallinity. (c) Comparison of the SEM and (d) EDX images of the fresh and 300-loops cycled samples.

4. CONCLUSIONS

In this work, we proposed a bimetallic nano oxygen carrier plus its scaled production. Methane reforming hydrogen production was achieved at mid-temperature of 500-600 °C. Over 95% conversion of CH₄ and H₂ concentration above 78% in the outlet was achieved at 600 °C. Furthermore, we proposed a method for scalable synthesis of the nano oxygen carrier and examined its performance under 600 °C and different S/C ratio. The typical performance of the 10-kg scale oxygen carrier was >90% conversion of CH₄ and >8 mL/min of H₂ yield per gram of oxygen carrier. In the longevity test, the 10-kg scale oxygen carrier maintained stable weight loss in 60-cycle TG test and nanoscale evenly distribution of Fe

and Ni in SEM-EDX characterization. Such results consolidated the potential of industrial application of nanoscale Fe-Ni bimetallic oxygen carrier in two-grade hydrogen production from chemical looping CH_4 reforming.

ACKNOWLEDGEMENT

The authors would like to acknowledge the support by National Natural Science Foundation of China (NSFC) (Grant No. 52206284, No. 51888103 and No.52241601).

DECLARATION OF INTEREST STATEMENT

The authors declare that they have no known competing financial interests or personal relationships that could have appeared to influence the work reported in this paper. All authors read and approved the final manuscript.

REFERENCES

[1] Adanez J, Abad A, Garcia-Labiano F, Gayan P, de Diego LF. Progress in Chemical-Looping Combustion and Reforming technologies. *Progress in Energy and Combustion Science*. 2012;38:215-82.

[2] Chuayboon S, Abanades S. An overview of solar decarbonization processes, reacting oxide materials, and thermochemical reactors for hydrogen and syngas production. *Int J Hydr Energy*. 2020;45:25783-810.

[3] Huang Z, He F, Chen D, Zhao K, Wei G, Zheng A, et al. Investigation on reactivity of iron nickel oxides in chemical looping dry reforming. *Energy*. 2016;116:53-63.

[4] Zeng L, Cheng Z, Fan JA, Fan L-S, Gong J. Metal oxide redox chemistry for chemical looping processes. *Nature Reviews Chemistry*. 2018;2:349-64.

[5] Tian M, Wang C, Han Y, Wang X. Recent Advances of Oxygen Carriers for Chemical Looping Reforming of Methane. *ChemCatChem*. 2021;13:1615-37.

[6] Zhu M, Chen S, Soomro A, Hu J, Sun Z, Ma S, et al. Effects of supports on reduction activity and carbon deposition of iron oxide for methane chemical looping hydrogen generation. *Appl Energy*. 2018;225:912-21.

[7] Saithong N, Authayanun S, Patcharavorachot Y, Arpornwichanop A. Thermodynamic analysis of the novel chemical looping process for two-grade hydrogen production with CO_2 capture. *Eng Convers Manage*. 2019;180:325-37.

[8] Kathe MV, Empfield A, Na J, Blair E, Fan L-S. Hydrogen production from natural gas using an iron-based chemical looping technology: Thermodynamic simulations and process system analysis. *Appl Energy*. 2016;165:183-201.

[9] Huang Z, Deng Z, Chen D, Wei G, He F, Zhao K, et al. Exploration of Reaction Mechanisms on Hydrogen Production through Chemical Looping Steam Reforming Using NiFe_2O_4 Oxygen Carrier. *ACS Sustainable Chemistry & Engineering*. 2019;7:11621-32.

[10] Yin X, Wang S, Sun R, Jiang S, Shen L. A Ce-Fe Oxygen Carrier with a Core-Shell Structure for Chemical Looping Steam Methane Reforming. *Industrial & Engineering Chemistry Research*. 2020;59:9775-86.

[11] Wei G, He F, Zhao Z, Huang Z, Zheng A, Zhao K, et al. Performance of Fe-Ni bimetallic oxygen carriers for chemical looping gasification of biomass in a 10 kWth interconnected circulating fluidized bed reactor. *Int J Hydr Energy*. 2015;40:16021-32.

[12] Lin Y, Zhang Z, Wang H, Fang S, Huang Z, Chen T, et al. An evaluation of the reactivity of synthetic Fe-Ni oxygen carriers: CO oxidation, H_2O reforming, and toluene cracking. *Eng Convers Manage*. 2021;240.

[13] Zhu Y, Jin N, Liu R, Sun X, Bai L, Tian H, et al. Bimetallic $\text{BaFe}_2\text{MAl}_9\text{O}_{19}$ (M = Mn, Ni, and Co) hexaaluminates as oxygen carriers for chemical looping dry reforming of methane. *Appl Energy*. 2020;258:114070.

[14] He X-M, Zhang C-W, Guo F-F, Yan S-M, Li Y-T, Liu L-Q, et al. Exchange-biased hybrid $\gamma\text{-Fe}_2\text{O}_3/\text{NiO}$ core-shell nanostructures: three-step synthesis, microstructure, and magnetic properties. *Phys Chem Chem Phys*. 2019;21:11967-76.

[15] Xue Z, Li L, Cao L, Zheng W, Yang W, Yu X. A simple method to fabricate $\text{NiFe}_2\text{O}_4/\text{NiO}@ \text{Fe}_2\text{O}_3$ core-shelled nanocubes based on Prussian blue analogues for lithium ion battery. *J Alloy Compd*. 2020;825:153966.

[16] Ma Z-Y, Yu Z-L, Xu Z-L, Bu L-F, Liu H-R, Zhu Y-B, et al. Origin of Batch Hydrothermal Fluid Behavior and Its Influence on Nanomaterial Synthesis. *Matter*. 2020;2:1270-82.

[17] Wang F, Qin XF, Meng YF, Guo ZL, Yang LX, Ming YF. Hydrothermal synthesis and characterization of $\alpha\text{-Fe}_2\text{O}_3$ nanoparticles. *Materials Science in Semiconductor Processing*. 2013;16:802-6.

[18] Jin Y, Chumanov G. Solution synthesis of pure 2H CuFeO_2 at low temperatures. *RSC Adv*. 2016;6:26392-7.

[19] Ishida M, Jin HG, Okamoto T. Kinetic behavior of solid particle in chemical-looping combustion: Suppressing carbon deposition in reduction. *Energy & Fuels*. 1998;12:223-9.